Electronic Supplementary Material (ESI) for CrystEngComm.

Supplementary Information

Cis-cyclodiphosph(V/V)azanes as Highly Stable and Robust Main Group Supramolecular Building Blocks

Davin Tan, Zi Xuan Ng, Ying Sim, Rakesh Ganguly, Felipe García*

School of Physical and Mathematical Sciences, Division of Chemistry and Biological Chemistry, Nanyang Technological University, 21 Nanyang Link 637371, Singapore (Singapore)

E-mail: fgarcia@ntu.edu.sg

- **Content.....1**
- **Experimental Section.....2**
- **Spectroscopic Data for compounds.....3**
- **Single Crystal X-ray Data and Description 6**
- **Computational Modeling……11**
- **References ……...14**

1. Experimental Section:

$^{31}P\{^{1}H\}$ ^{1}H and ^{13}C NMR spectra were recorded on a BRUKER AVANCE III 300 MHz with chemical shifts (δ) given in parts per million (ppm). Deuterated $CDCl_3$ was used as the NMR solvent. Single crystal X-ray diffraction data was collected on a Bruker X8 CCD Diffractometer and/or Bruker Kappa CCD Diffractometer. The reflections were recorded and processed with Bruker SAINT software package which uses narrow-frame algorithm. The structures were solved via direct methods with the SHELXTL software package and refined by full-matrix least-squares calculations on F2 with anisotropic displacements parameters assigned to all atoms. Fourier-transform Infra-red (FTIR) spectroscopy was performed on an Attenuated Total Reflectance (ATR) setup

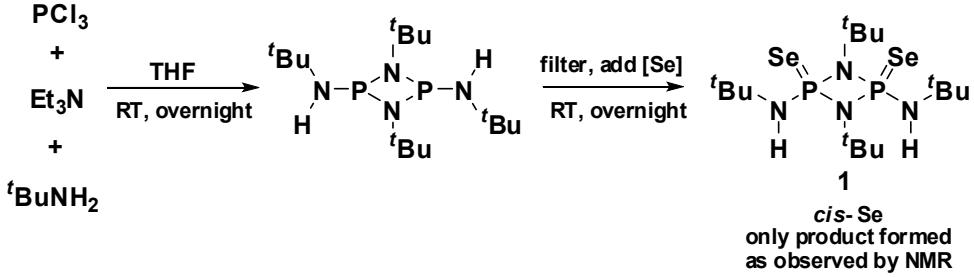

Figure S1. General scheme for the two-step synthesis of compound **1**.

Synthesis of **1**: 5mmol of distilled PCl_3 and 10mmol of distilled Et_3N was added to a 500mL two neck round bottom flask containing 250mL of dry THF as the solvent. The flask was charged with Ar gas and cooled using a mixture of dry ice in acetone. Another solution mixture containing 10mmol of distilled $^{t}BuNH_2$ in 50mL of dry THF was added drop wise to the previous mixture *via* a dropping funnel, over a period of 1 hour. Formation of a white precipitate was observed. The reaction was then allowed to stir overnight at room temperature. Next, the reaction mixture was filtered to remove the white solids and the filtrate was transferred to a 350mL Schlenk flask and the solvent was removed *in vacuo* until the mixture was about 150mL. 11mmol of elemental Se was added to the solution and allowed to stir overnight at room temperature. Excess unreacted Se was removed by filtration and the filtrate was collected and transferred to a 250mL round bottom flask. The remaining solvent was removed using a rotator evaporator and the desired pure product, compound **1** was obtained as an off-white solid.

Stability test: Compound **1** was dissolved in THF and the solution was placed in an NMR tube. A few drops of distilled water was added and the mixture was left to stand at ambient temperature and exposed to air. After 21 days, the NMR spectrum of the mixture was recorded.

To obtain single crystals of the all the compounds for single-crystal X-ray diffraction measurements, the various compounds were dissolved in different solvents, passed through a PTFE filter to remove any solid particles and left to evaporate over several days in a small 5mL dram vial, on the benchtop. Please refer to main manuscript for list solvents and combination of solvents used. The solvents used were not pre-treated or dried in any particular manner.

2. Spectroscopic Data

Compound 1

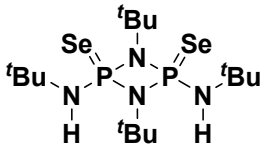

White solid (88% yield); **^{1}H-NMR** (300 MHz, $CDCl_3$) δ 1.45 (s, 18H), δ 1.73 (s, 18H), δ2.98 (s, 1H), δ3.35 (s, 1H); **^{13}C-NMR** (75 MHz, $CDCl_3$) δ 30.0, 31.6, 55.8, 58.3. **^{31}P{^{1}H}-NMR:** δ 26.0. **HRMS**: obtained for $C_{16}H_{39}N_4P_2Se_2$ [M+H$^+$], calculated: 509.0980, measured: 509.0992.

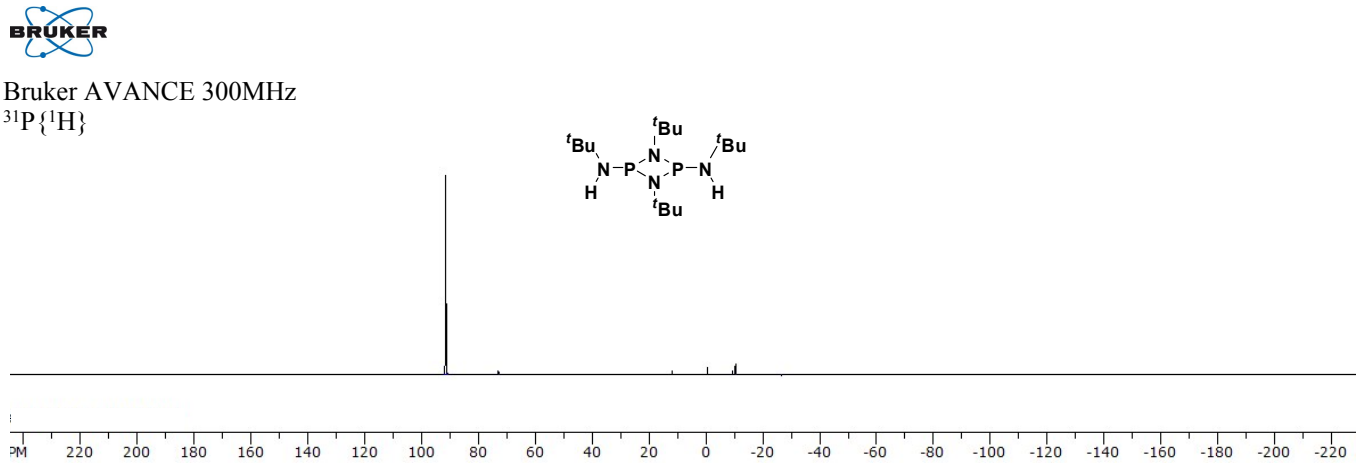

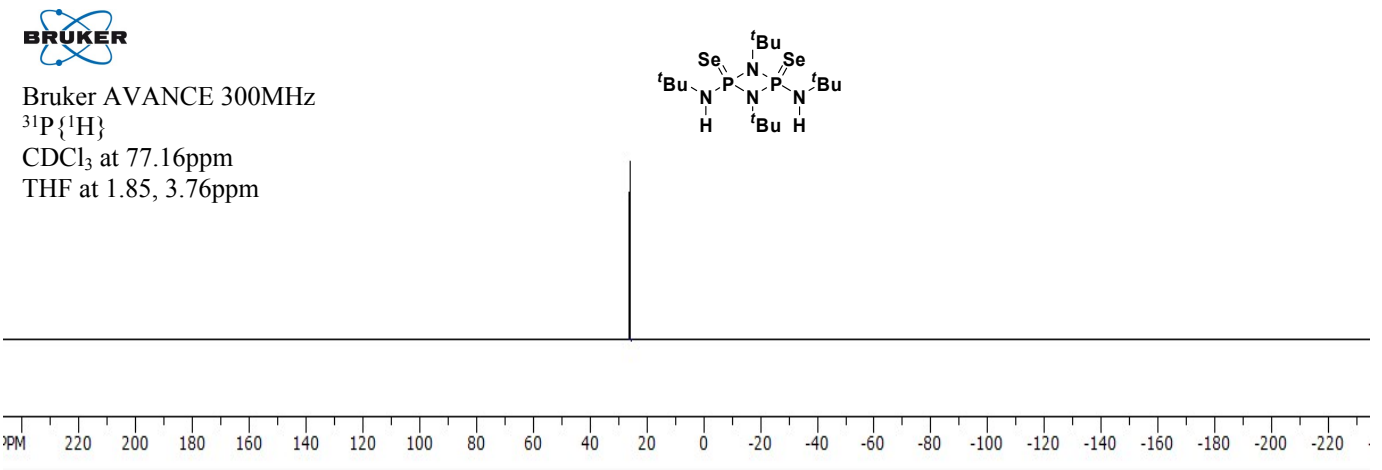

Figure S2. Comparison of the *in situ* ^{31}P{^{1}H} of the intermediate before oxidation and compound **1**, after oxidation, shows only one resonance signal, denoting that only one product is formed (either *cis*-Se or *trans*-Se). SC-XRD data from single crystals obtained after recrystallization revealed that only the *cis*-Se was formed.

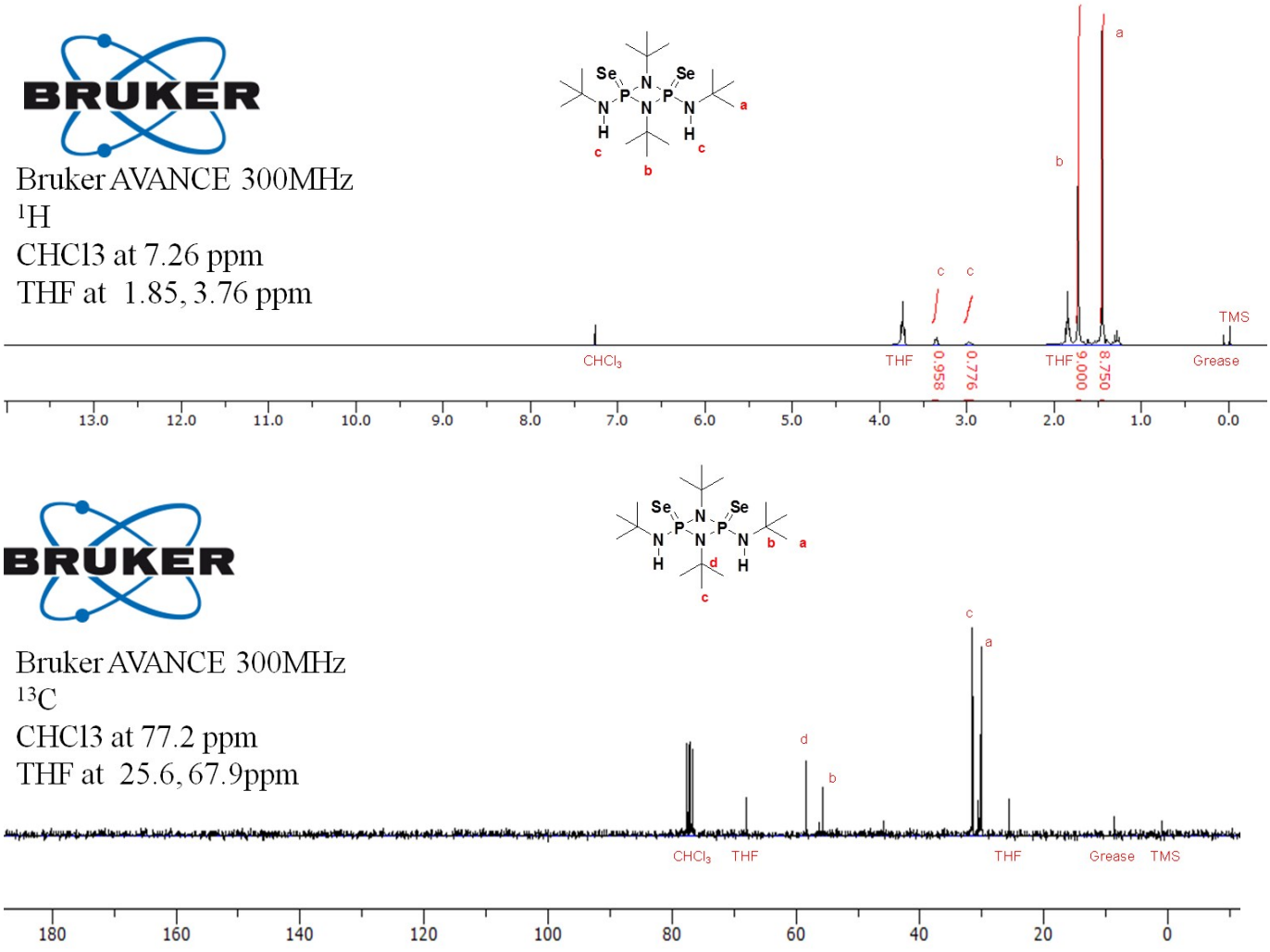

Figure S3. ^{1}H and ^{13}C NMR spectrum of compound **1**.

O_2 and H_2O stability test

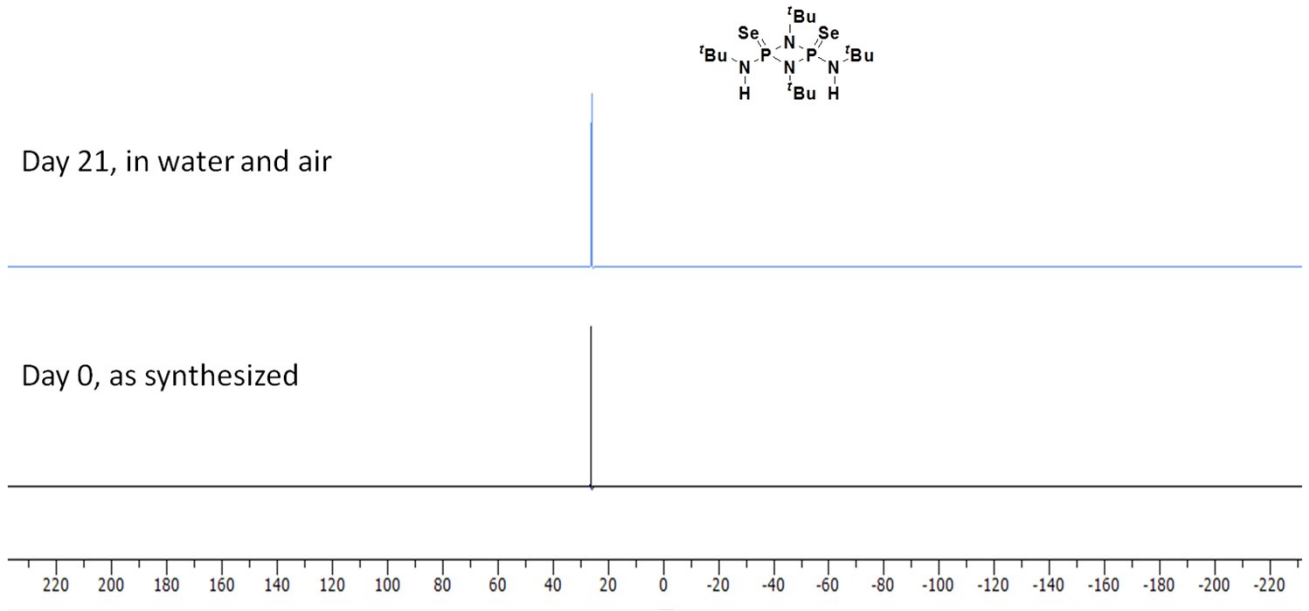

Figure S4. Comparison of the $^{31}P\{^{1}H\}$ NMR spectra of compound **1** before and after exposure to water and oxygen for 21 days.

Analysis of the proton-decoupled phosphourus $^{31}P\{^{1}H\}$ NMR spectrum of **1** after exposure to water and oxygen (on the benchtop) for 21 days revealed that the compound is highly robust and showed no signs of decomposition or hydrolysis to form phosphoric acid. This demonstrates how pre-emptive oxidation using Se can be a useful strategy to form highly stable cyclophosphaz(V)anes that allows them to be suitable candidates to be used as main group based supramolecular building blocks.

Fourier Transform Infra Red Attenuated Total Reflectance Spectroscopic data of 1

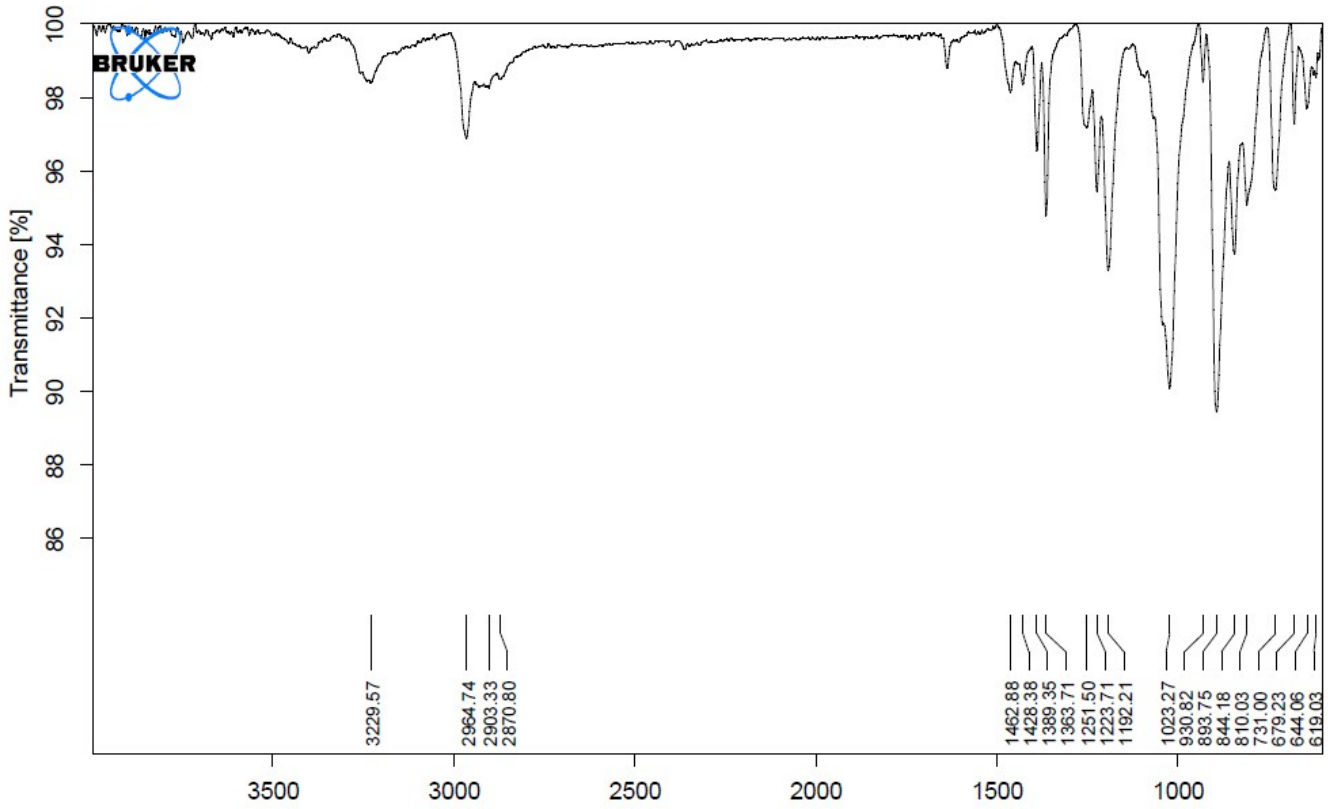

Figure S5. FTIR-ATR data of **1**.

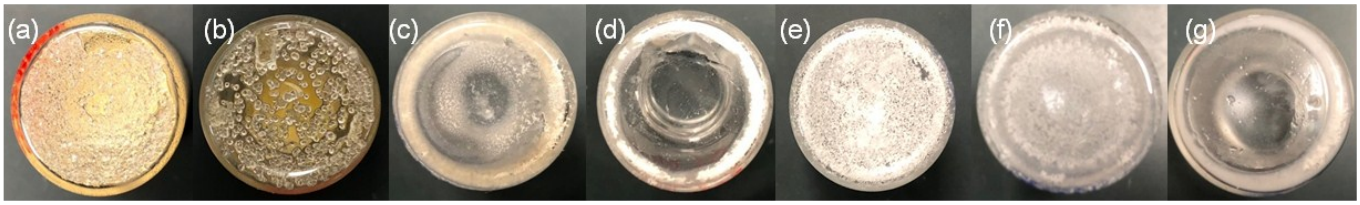

Figure S6. A sampling of pictures of the single crystals and films of **1** obtained by slow evaporation of various solvents: (a) DMSO, (b) acetone, (c) $CHCl_3$, (d) THF, (e) DCM, (f) hexane, and (g) diethylether and $CHCl_3$ mixture.

X-ray diffraction quality crystals, similar to those shown in Figure S6(a) and S6(b), were obtained for the solvents mentioned in Table 1. Various films were obtained for the other solvents and solvent combinations. The films are formed at the bottom of the vials, and are either hard crusts, as shown in S6(d), S6(e) and S6(f), or a less crusty consistency like in S6(c) and S6(g). X-ray diffraction quality crystals were not obtained for these solvents and solvent combinations. FTIR-ATR spectroscopic data obtained for these films showed the presence of compound **1** for the hard crust-like films and less crusty films and compared with crystals obtained with the DMSO solvate.

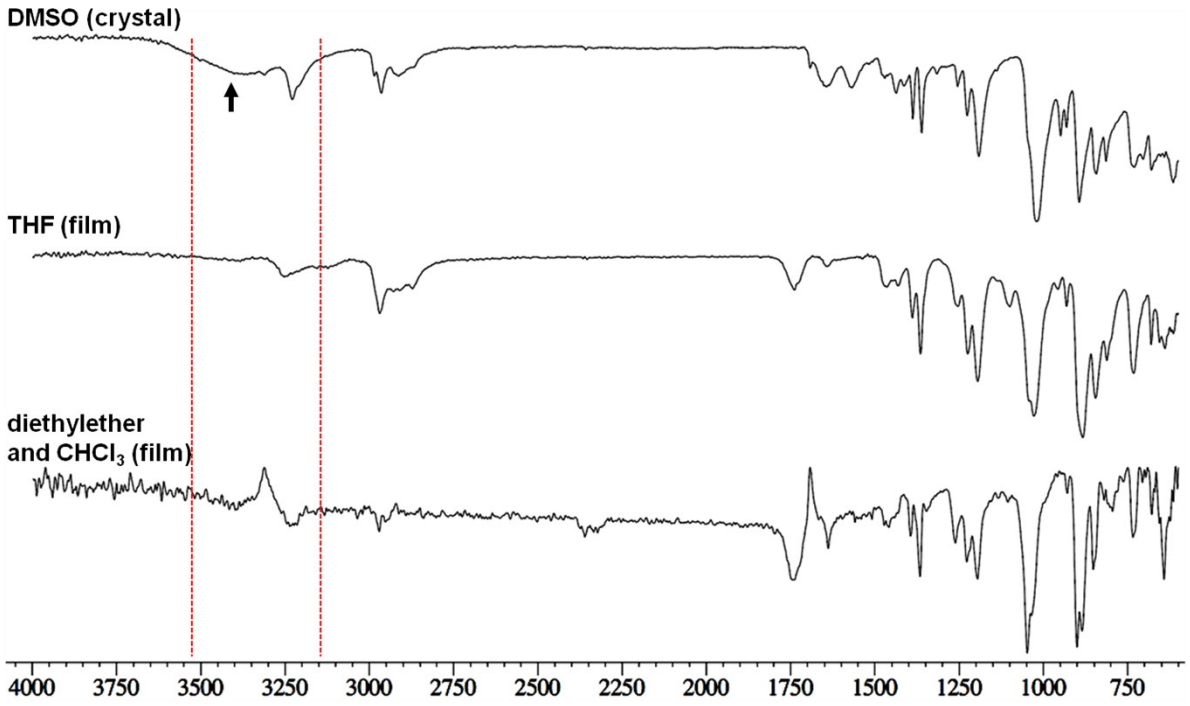

Figure S7. Comparison of the FTIR spectrum of the solvate crystals of DMSO and THF and diethylether with $CHCl_3$ films of **1**.

The N-H stretching region is shown between the red dotted lines and the black arrow denotes a visible broad peak at 3401 cm^{-1} which might be due to the formation of bifurcated hydrogen bond.

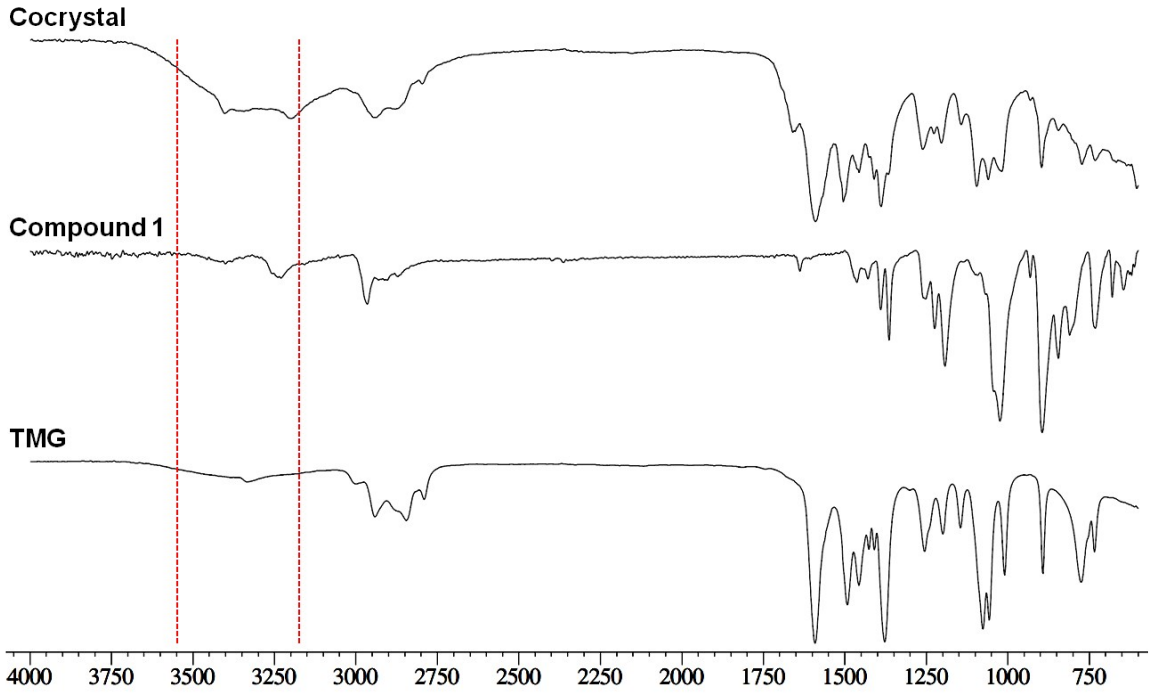

Figure S8. Comparison of the FTIR spectrum of the TMG, compound **1** and their cocrystal.

The N-H stretching region is shown between the red dotted lines and denotes a broadening with several new peaks.

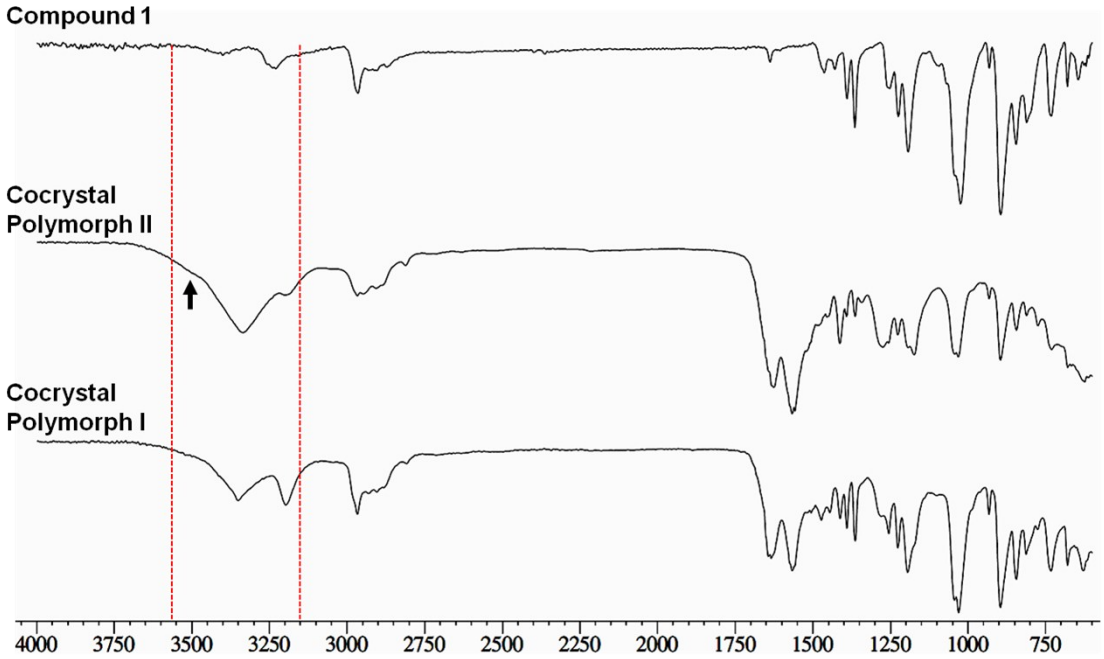

Figure S9. Comparison of the FTIR spectrum of the compound **1** and the two different cocrystal polymorphs with DMU.

The N-H stretching region is shown between the red dotted lines and the black arrow denotes a slight shoulder at 3573 cm^{-1} which is suspected to caused by the Y_2 interaction.

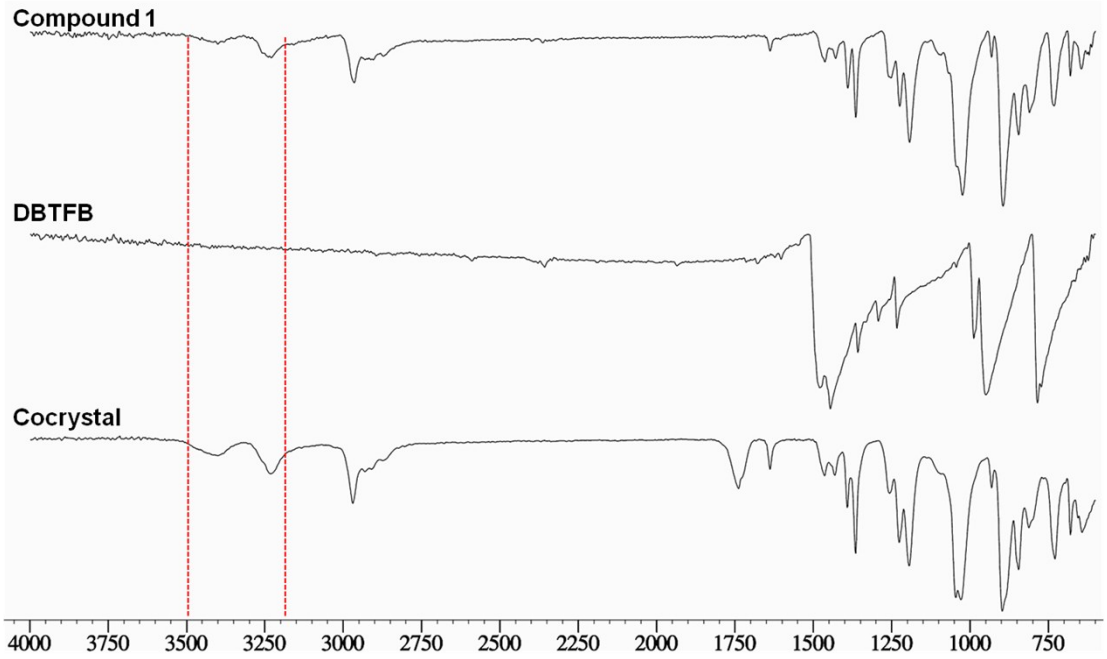

Figure S10. Comparison of the FTIR spectrum of the compound **1**, DBTFB and the cocrystal polymorphs with DMU.

The N-H stretching region is shown between the red dotted lines which did not show significant change between compound **1** and its cocrystal with DBTFB, which is expected since the molecules are linked by intermolecular halogen-bonding interactions.

4. Single Crystal X-ray Data and Description

Table S1. X-ray crystallographic data.

Compound	acetone solvate	DMSO solvate	DMF solvate	MeOH solvate
Formula	$C_{19}H_{44}N_4OP_2Se_2$	$C_{18}H_{42}N_4SOP_2Se_2$	$C_{19}H_{44}N_5OP_2Se_2$	$C_{17}H_{42}N_4OP_2Se_2$
MW	566.44 g/mol	585.30 g/mol	578.45 g/mol	538.40 g/mol
Temperature	240(2) K	100(2) K	100(2) K	100(2) K
Wavelength	0.71073 Å	0.71073 Å	0.71073 Å	0.71073 Å
Crystal system	orthorhombic	orthorhombic	orthorhombic	monoclinic
Space group	*P* nma	*P* n m a	*P* n m a	*P* 2_1/c
Unit cell	a = 20.570(3) Å	a = 20.6757(4) Å	a = 21.8437(6) Å	a = 11.2306(5) Å
	b = 11.104(2) Å	b = 10.9903(2) Å	b = 10.7274(3) Å	b = 15.1878(6) Å
	c = 12.117(2) Å	c = 11.8544(2) Å	c = 11.5787(4) Å	c =15.8046(6) Å
	α = 90°	α = 90°	α = 90°	α = 90°
	β = 90°	β = 90°	β = 90°	β = 107.6355(14)°
	γ = 90°	γ = 90°	γ = 90°	γ = 90°
Volume	2767.6(8) Å^3	2693.70(8) Å^3	2713.19(14) Å^3	2569.07(18) Å^3
Z	4	4	4	4
Density	1.355 g/cm^3	1.443 g/cm^3	1.416 g/cm^3	1.392 g/cm^3
Abs. coeff.	2.803 mm^{-1}	3.204 mm^{-1}	2.863 mm^{-1}	3.016 mm^{-1}
F(000)	1168	1212	1196	1112
Theta min-max	2.68 to 32.06°	2.71 to 30.99°	2.75 to 31.03°	2.38 to 33.16°
Reflections	7676	51161	41818	56299
Restraints/para.	191 / 171	0/151	55/183	0/249
Goodness of Fit S	0.984	0.956	1.073	0.988
R final R1/wR2	0.0384/0.0849	0.0187/0.0456	0.0278/0.0527	0.0414/0.0807
Peak/hole	0.847/-0.545	0.429/-0.372	0.465/-0.345	0.632/-0.878
tBut ring, terminal	eclipse, eclipse	eclipse, eclipse	eclipse, eclipse	staggered, eclipse
Bifurcation bite angle	82.0°	85.6°	85.5°	86.0 °

CH_3CN solvate	DMU polymorph 1	DMU polymorph 2	TMG	1,4-dibromo-tetrafluorobenzene
$C_{18}H_{41}N_5P_2Se_2$	$C_{57}H_{138}N_{18}O_3P_6Se_6$	$C_{19}H_{46}N_6OP_2Se_2$	$C_{21}H_{51}N_7P_2Se_2$	$C_{22}H_{38}Br_2F_4N_4P_2Se_2$
547.42 g/mol	1783.43 g/mol	594.48 g/mol	621.54g/mol	814.24 g/mol
100(2) K	100(2) K	100(2) K	100(2) K	100(2) K
0.71073 Å	0.71073 Å	0.71073 Å	0.71073 Å	0.71073 Å
monoclinic	orthorhombic	monoclinic	orthorhombic	monoclinic
P 2_1/c	*P* n a 2_1	*P* 2_1/c	*P* b c a	*P*2_1/m
a = 10.6563(6) Å	a = 50.3437(18) Å	a = 17.5948(3) Å	a = 16.1497(14) Å	a = 9.1510(2) Å
b = 11.7263(6) Å	b = 17.1420(5) Å	b = 17.2259(3) Å	b = 23.108(2) Å	b = 16.1119(3) Å
c = 21.0354(10) Å	c = 10.2119(3) Å	c = 18.9346(4) Å	c = 33.223(3) Å	c = 11.5547(2) Å
α = 90°	α = 90°	α = 90°	α = 90°	α = 90°
β = 91.800(2)°	β = 90°	β = 91.9478(8)°	β = 90°	β = 112.9078(7)°
γ = 90°	γ = 90°	γ = 90°	γ = 90°	γ = 90°
2627.3(2) Å^3	8812.8(5) Å^3	5735.50(19) Å^3	12398.4(18) Å^3	1569.26(5) Å^3
4	4	8	16	2
1.384 g/cm^3	1.344 g/cm^3	1.377 g/cm^3	1.332 g/cm^3	1.723 g/cm^3
2.949 mm^{-1}	2.647 mm-1	2.711 mm^{-1}	2.510 mm^{-1}	5.047 mm^{-1}
1128	3696	2464	5184	804
2.74 to 37.80°	2.32 to 30.09°	2.46 to 32.04°	2.40 to 31.04°	2.29 to 33.15°
14312	103996	127003	262083	38719
0/258	1949/1082	0/569	2/616	2/188
1.060	1.013	1.004	1.025	1.027
0.0521/0.1108	0.0293/0.0556	0.0347/0.0625	0.0341/0.0717	0.0235/0.0499
0.867/-1.305	0.517/-0.538	0.581/-0.485	0.646/-1.364	0.739/-0.784
eclipse, eclipse	eclipse, eclipse	eclipse, eclipse	eclipse, eclipse	eclipse, endo
76.8°	89.8°	88.4°	86.6°	69.9°

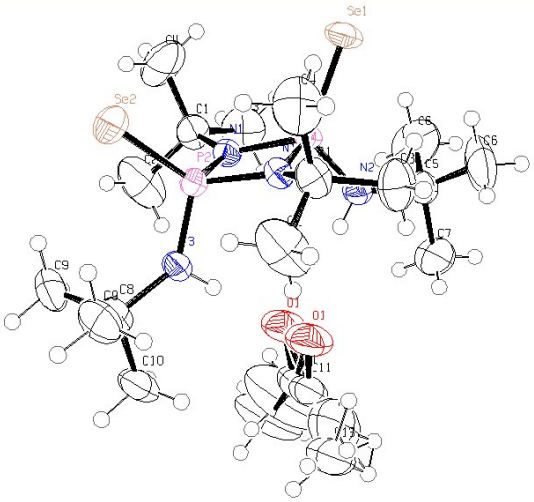

Figure S11. Acetone solvate of **1**, visualized using ORTEP-3, with thermal ellipsoids set at 50% probability. The molecule of acetone is disordered over two positions. CCDC code 1829236.

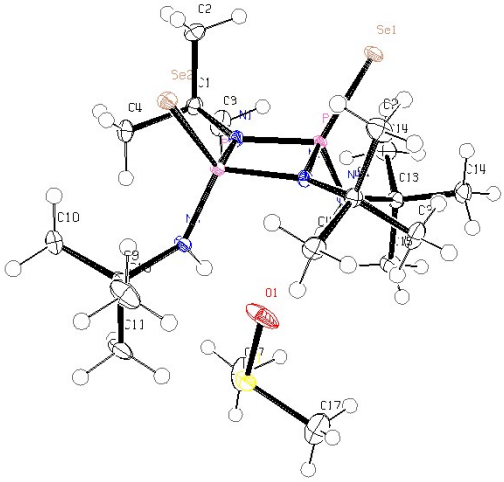

Figure S12. DMSO solvate of **1**, visualized using ORTEP-3, with thermal ellipsoids set at 50% probability. CCDC code 1829228.

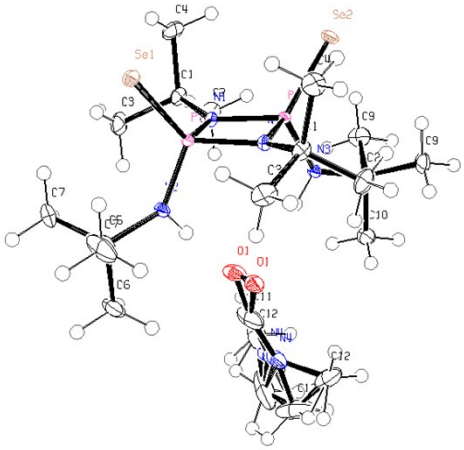

Figure S13. DMF solvate of **1**, visualized using ORTEP-3, with thermal ellipsoids set at 50% probability. The molecule of DMF is disordered over two positions. CCDC code 1829230.

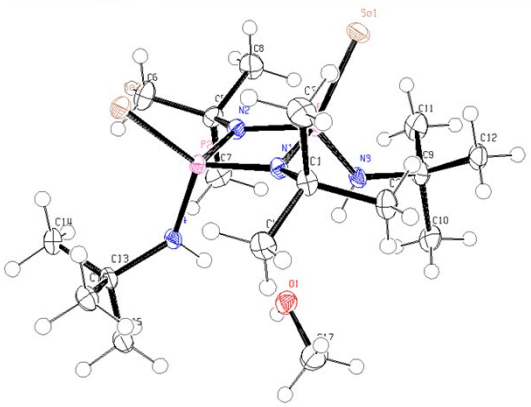

Figure S14. MeOH solvate of **1**, visualized using ORTEP-3, with thermal ellipsoids set at 50% probability. CCDC code 1829229.

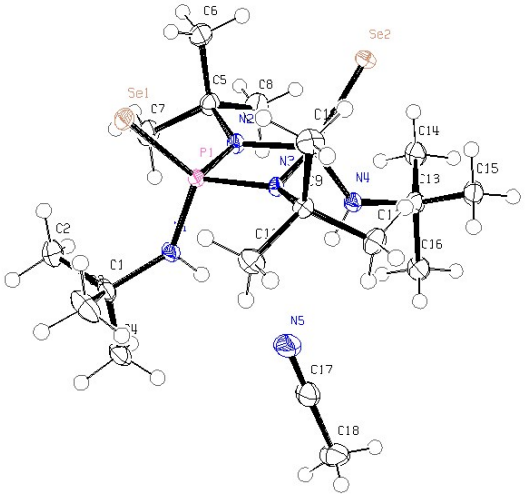

Figure S15. CH_3CN solvate of **1**, visualized using ORTEP-3, with thermal ellipsoids set at 50% probability. CCDC code 1829233.

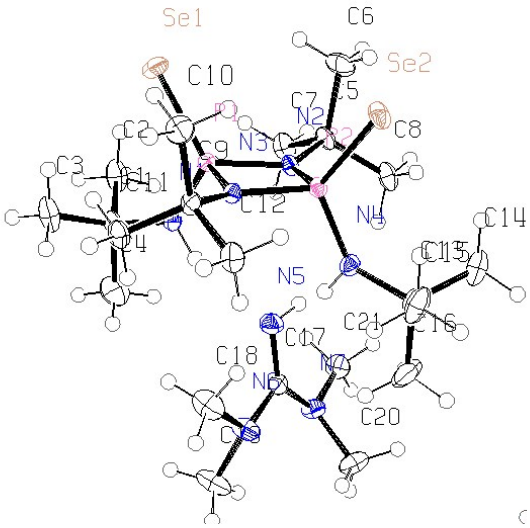

Figure S16. Cocrystal of TMG with **1**, visualized using ORTEP-3, with thermal ellipsoids set at 50% probability. CCDC code 1829235.

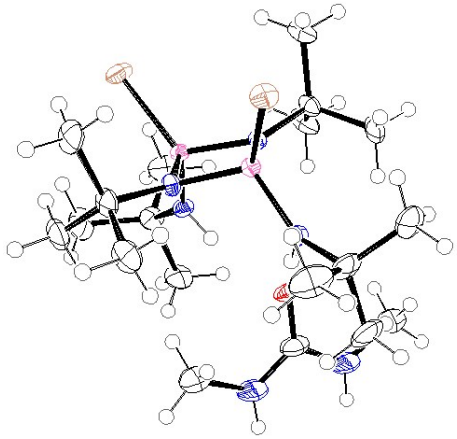

Figure S17. Polymorph I of cocrystal of DMU with **1**, visualized using ORTEP-3, with thermal ellipsoids set at 50% probability. CCDC code 1829231.

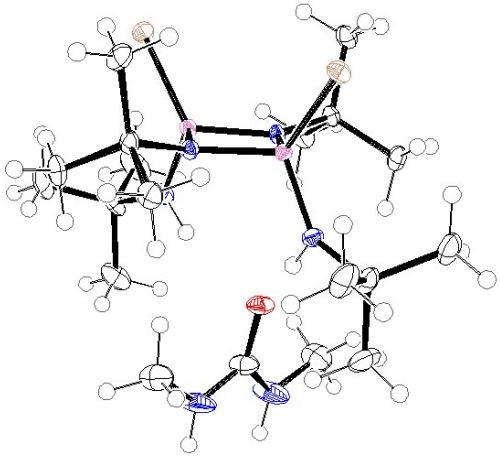

Figure S18. Polymorph II of cocrystal of DMU with **1**, visualized using ORTEP-3, with thermal ellipsoids set at 50% probability. CCDC code 1829232.

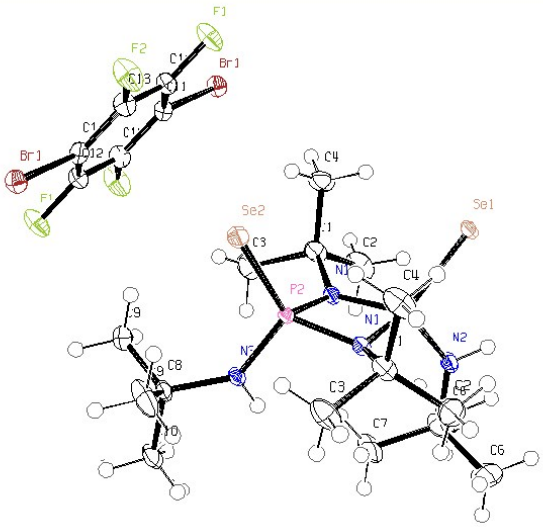

Figure S19. Cocrystal of DBTFB with **1**, visualized using ORTEP-3, with thermal ellipsoids set at 50% probability. CCDC code 1829234.

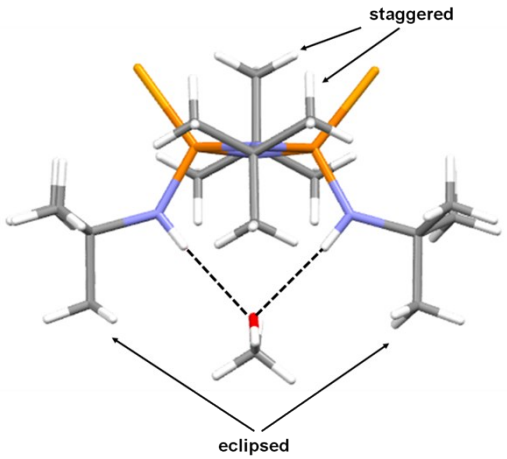

Figure S20. Side by side comparison of the MeOH solvate of **1**, illustrating the staggered (terminal) and eclipsed (ring) *t*-butyl groups.

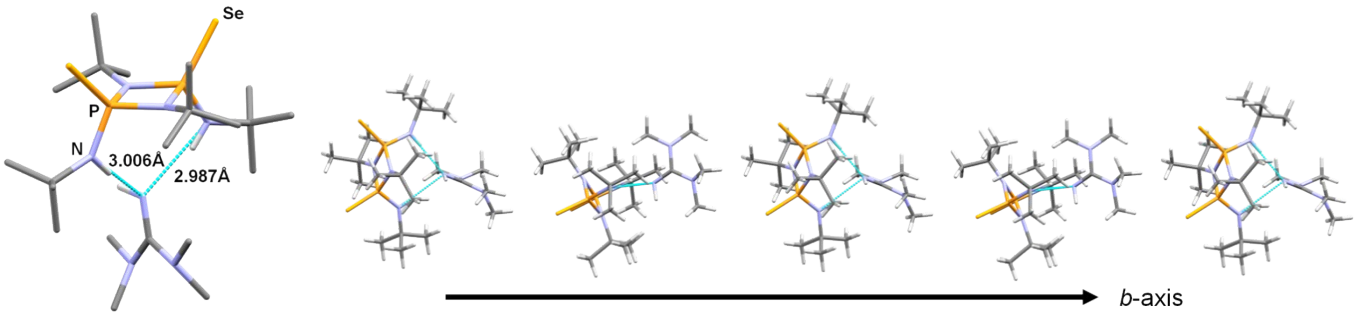

Figure S21. Ball-and-stick representation of the cocrystal of TMG and **1** (left), and its molecular packing (right).

Analysis of the crystal structure revealed that the TMG molecule is not protonated *i.e.* it is neutral. Molecular packing of the cocrystal shows alternating molecules of **1** and TMG, in which each associated pair is rotated about 90° with each other as it propagates along the crystallographic *b*-axis. The cocrystals of TMG:**1** can be obtained by slow evaporation of 1:1 solution mixtures using either acetone, $CHCl_3$, CH_2Cl_2 or THF as the solvent.

5. Computational Modelling

Density functional theory calculations were performed, based on the Cartesian coordinates derived from SCXRD data, by employing the Gaussian 09 package of programs.[1] Calculations were carried out using the popular Becke's three parameter functional[2] with the nonlocal Lee-Yang-Parr correlation functional[3] (B3LYP) theory. LANL2DZ basis set including double-ζ valence basis set with the Hay and Wadt effective core potential[4] (ECP) was used for the heavy Br and Se atoms, while the 6-31+G(d,p) Pople basis set[4] was used for the rest of the atoms. All calculations were performed in the gas phase. Electrostatic surface potential of the halogen bonded cocrystal of compound **1** with DBTFB was then modelled using the "cubegen" keyword based on the formatted checkpoint file (checkpoint file generated during gas phase calculation), using the self-consistent field (SCF) density and with *medium* 6 points/Bohr grid for the cubes.

5. References

[1] M. J. Frisch, G. W. Trucks, H. B. Schlegel, G. E. Scuseria, M. A. Robb, J. R. Cheeseman, G. Scalmani, V. Barone, B. Mennucci, G. A. Petersson, H. Nakatsuji, M. Caricato, X. Li, H. P. Hratchian, A. F. Izmaylov, J. Bloino, G. Zheng, J. L. Sonnenberg, M. Hada, M. Ehara, K. Toyota, R. Fukuda, J. Hasegawa, M. Ishida, T. Nakajima,, Y. Honda, O. Kitao, H. Nakai, T, Vreven, J. J. A. Montgomery, J. E. Peralta, F.,Ogliaro, M. Bearpark, J. J. Heyd, E. Brothers, K. N. Kudin, V. N. Staroverov, R, Kobayashi, J. Normand, K. Raghavachari, A. Rendell, J. C. Burant, S. S. Iyengar, J. Tomasi, M. Cossi, N. Rega, N. J. Millam, M. Klene, J. E. Knox, J. B. Cross, V. Bakken, C. Adamo, J. Jaramillo, R. Gomperts, R. E. Stratmann, O. Yazyev, A. J. Austin, R. Cammi, C. Pomelli, J. W. Ochterski, R. L. Martin, K., Morokuma, V. G. Zakrzewski, G. A. Voth, P. Salvador, J. J. Dannenberg, S. Dapprich, A. D.Daniels, Ö Farkas, J. B. Foresman, J. V. Ortiz, J. Cioslowski, D. J. Fox, *Gaussian 09, revision D.01*, Gaussian, Inc.: Wallingford, CT, **2009**.

[2] A. D. Becke, *J. Chem. Phys.*, **1993**, *98*, 5648.

[3] C. Lee, W. Yang, R. G. Parr, *Phys. Rev. B*, **1988**, *37*, 785.

[4] P. J. Hay, W. R. Wadt, *J. Chem. Phys.*, **1985**, *82*, 299.

[5] R. Ditchfield, W. J. Hehre, J. A. Pople, *J. Chem. Phys.*, **1971**, *54*, 720.